Key Words:	Renal cell carcinoma, prognostic marker, MUC13, proliferation, apoptosis, NFκB, sorafenib, sunitinib

MUC13 overexpression in renal cell carcinoma plays a central role in tumour progression and drug resistance

Yonghua Sheng[1], Choa Ping Ng[1#], Rohan Lourie[1#], Esha T. Shah[2,3#], Yaowu He[4], Kuan Yau Wong[1], Inge Seim[2,3], Iulia Oancea[1], Christudas Morais[5], Penny L. Jeffery[1,2,3], John Hooper[4], Glenda C. Gobe[5*], Michael A. McGuckin[1*]

1. Inflammatory Disease Biology and Therapeutics Group, Mater Research Institute – The University of Queensland, Translational Research Institute, Brisbane, Queensland 4102, Australia; 2. Ghrelin Research Group, Translational Research Institute-Institute of Health and Biomedical Innovation, Queensland University of Technology, Brisbane, QLD 4102, Australia; 3. Comparative and Endocrine Biology Laboratory, Translational Research Institute-Institute of Health and Biomedical Innovation, Queensland University of Technology, Brisbane, QLD 4012, Australia; 4. Cancer Biology Group, Mater Research Institute-University of Queensland, Brisbane, Queensland 4101, Australia; 5. Centre for Kidney Disease Research, The University of Queensland School of Medicine, Translational Research Institute, Brisbane, QLD 4102, Australia

[#]Equal second authors
*Equal senior authors

Correspondence: **Prof. Michael McGuckin**
Mater Research Institute
University of Queensland
37 Kent St
Woolloongabba, Brisbane, QLD 4102, Australia
P: +61 7 3443 7623
F: +61 7 3163 2550
M: 0439 747001
Email: michael.mcguckin@mater.uq.edu.au

and

Prof. Glenda C Gobe
School of Medicine
University of Queensland
Translational Research Institute
37 Kent Street
Woolloongabba, Brisbane, QLD 4102, Australia
Phone 61 7 344 38011
Mobile 61 (0) 438 755 416
Email g.gobe@uq.edu.au

Running title: MUC13 in Renal Cell Carcinoma

Novelty & Impact Statements: New prognostic markers and therapeutic targets are needed for renal cell carcinoma (RCC). MUC13 mucin is overexpressed by gastrointestinal tumors but its significance in RCC is unknown. The authors show MUC13 is aberrantly expressed and associated with poor survival in RCC. MUC13 promotes growth, blocks apoptosis, and silencing sensitises to killing by kinase inhibitors and reverses drug resistance. Thus, MUC13 is a new prognostic marker for aggressive early stage RCC and a new therapeutic target.

Abbreviations used in this paper: RCC, Renal cell carcinoma; NFκB, nuclear factor-kappa-B; siRNA, small interfering RNA.

Conflict of interests: There are none to declare.

ABSTRACT

Metastatic renal cell carcinoma is a largely incurable disease, and existing treatments targeting angiogenesis and tyrosine kinase receptors are only partially effective. Here we reveal that MUC13, a cell surface mucin glycoprotein, is aberrantly expressed by most renal cell carcinomas, with increasing expression positively correlating with tumor grade. Importantly, we demonstrated that high MUC13 expression was a statistically significant independent predictor of poor survival in two independent cohorts, particularly in stage 1 cancers. In cultured renal cell carcinoma cells MUC13 promoted proliferation and induced the cell cycle regulator, cyclin D1, and inhibited apoptosis by inducing the anti-apoptotic proteins, BCL-xL and survivin. Silencing of *MUC13* expression inhibited migration and invasion, and sensitised renal cancer cells to killing by the multi-kinase inhibitors used clinically, sorafenib and sunitinib, and reversed acquired resistance to these drugs. Furthermore, we demonstrated that MUC13 promotion of renal cancer cell growth and survival is mediated by activation of nuclear factor κB, a transcription factor known to regulate the expression of genes that play key roles in the development and progression of cancer. These results show that MUC13 has potential as a prognostic marker for aggressive early stage renal cell cancer and is a plausible target to sensitise these tumours to therapy.

Keywords: MUC13; Renal cell carcinoma; prognostic marker; proliferation, apoptosis sorafenib, sunitinib, NFκB

Introduction

Renal cell carcinoma (RCC) comprises approximately 4% of all cancers, but an alarming increase in incidence has been reported,[1] with an estimated 338,000 new cases and 102,000 deaths annually.[2] The main histologic subtype, clear cell RCC (ccRCC), accounts for 75% of all cases.[3] Approximately 30% of RCC patients present with metastatic disease at the time of diagnosis and nearly half of the remainder will subsequently develop, and ultimately die from, metastasis.[4] Major clinical challenges for RCC are the lack of a screening method for early-stage diagnosis, the lack of biomarkers for prediction of progression, the frequent development of metastatic disease to the lung, lymph nodes, bone, liver and brain, and the lack of efficacy of therapy for metastatic disease because of inherent or developing drug resistance. RCC is poorly responsive to chemotherapy due to the development of multi-drug resistance. Antiangiogenic agents, tyrosine kinase inhibitors such as sorafenib and sunitinib which affect both angiogenesis and tumour growth and survival pathways, and immunotherapy are the major current approaches for patients with advanced RCC. Unfortunately, while 10-20% of patients have tumors that are initially refractory to therapy, a large majority relapse after a median of 10-12 months.[5] Recently, a definitive phase 3 trial found that sorafenib or sunitinib provided no disease-free survival benefit compared to placebo despite substantial toxicity.[6] Taken together, there is a great need to identify new diagnostic and prognostic markers, as well as developing novel therapeutic strategies for treatment of advanced RCC.

Mucins are complex cell surface and secreted glycoproteins that provide protection and lubrication to the epithelial surface of mucosal tissues.[7-9] Alterations in the expression and glycosylation of cell surface mucins occur in multiple types of adenocarcinoma. The advantage of their expression in these cancers is likely linked to their functions in healthy tissue, promoting epithelial resistance and resilience to toxic challenges at mucosal surfaces.[9] Carcinoma cells derived from epithelia overexpress mucins to exploit their role in promoting growth, survival, migration and invasion of cancer cells.[8, 9] Mucins have thus been identified as markers of poor prognosis[10, 11] and as attractive therapeutic targets[12-19] in many cancers.

The MUC13 cell surface mucin is overexpressed in gastric,[20] colorectal,[21-23] pancreatic[24, 25] and ovarian[26] cancers. Normally this protein is expressed on the apical

borders of epithelial cells of the intestine, including the luminal surface glycocalyx of enterocytes and goblet cells in the small and large intestine,[27] with increased cytoplasmic expression seen in response to infection [28] and inflammation.[29] MUC13 has a relatively short 151-amino acid extracellular domain compared with other cell surface mucins, three epidermal growth factor (EGF)-like domains, one sea urchin sperm protein enterokinase arginine (SEA) domain within an extracellular component, followed by a short 23-amino acid transmembrane domain and a 69- amino acid cytoplasmic domain that includes eight serine and two tyrosine residues for potential phosphorylation. In addition, there is a protein kinase C consensus phosphorylation motif [27] that could play a role in cell signaling pathways and promote proliferation and cell survival.[22, 26, 27, 29] Recently, we reported that cytoplasmic MUC13 expression is elevated in high grade and metastatic colorectal cancer, and that MUC13 promotes activation of nuclear factor κB (NFκB), is anti-apoptotic,[30] and pro-inflammatory [31] – rendering MUC13 a potential therapeutic target.[30] However, the functional significance of MUC13 in renal neoplasms has not been defined, and therefore its potential prognostic and therapeutic significance in RCC remains unknown. In this study, we set out to investigate the biological and clinical relevance of MUC13 and its tumorigenic properties in RCC, aiming to develop better treatments for this cancer.

Materials and Methods

Clinical samples

A total of 244 patients from 5 distinct cohorts were used for this study. The clinical data are presented in Supplementary Table 1. All patients in cohorts 1 to 4 gave informed consent for their participation in the research. This study was approved by the PAH Human Research Ethics Committee (PAH HREC Approval 2006/189). Cohort 1 included 10 patients with ccRCC, cohort 2 included 8 patients with 6 ccRCC and 2 papillary RCC, cohort 3 included 12 patients with ccRCC and cohort 4 included 124 patients with 110 ccRCC (35 patients with survival data) and 14 papillary and chromophobe RCC. Additionally, ccRCC tissue microarray (#HKid-CRC180Sur-01; 90 cases, cohort 5) with survival data (81 patients) clinical stage (75 patients) was purchased from US Biomax, Inc. (Biomax, Rockville, MD, USA)

Cell culture, transfection and infection

ALL RCC and HEK293 cell lines were obtained from the American Type Culture Collection (ATCC, Rockville, MD, USA). 786-O and 769-P (both are VHL–deficient) were propagated in RPMI-1640 (Life Technologies, Carlsbad, CA, USA) whereases ACHN (WT for *VHL)*, A489, A704 (both are VHL–deficient) and HEK293 were propagated in DMEM (Life Technologies) with 10% heat inactivated fetal calf serum, 100 µg /mL penicillin, 100 µg/mL streptomycin, and 2 mM L-glutamine. All the cell lines have been tested for their STR DNA profiling and the origin and identity of the cells have been confirmed.

Two siRNAs (#1 is a SMART pool and #2 is a distinct individual siRNA against the target sequence CUCAGCUGAUGCUGUAACA) targeting *MUC13* and non-targeted control siRNA were purchased from Dharmacon (Dharmacon Research, Lafayette, CO, USA). Oligonucleotide transfection was performed with Lipofectamine 2000 Reagent (Life Technologies) at a final concentration of 50 nM. For stable clones, $5x10^6$ amphotropic (PA317) packaging cells were transfected with 10 µg DNA of the appropriate retroviral construct (pRUFneo) by Lipofectamine 2000 Reagent (Life Technologies) according to the manufacturer's protocol. Culture supernatants were collected 36-48 h after transfection and filtered through 0.45 µm filter. HEK293 cells were infected with the filtered viral supernatants in the presence of 4 µg/ml polybrene (Sigma-Aldrich) for 12 h, after which the medium was changed. Fresh viral suspensions were added after a 24 h interval for an additional 12 h. Infected cells were selected for 10 days in 400 µg ml^{-1} G418 and maintained in 100 µg ml^{-1} G418.

Immunohistochemistry

The expression of MUC13 was analyzed by immunohistochemistry (IHC) with the anti-MUC13 polyclonal antibody - R20C1 (dilution, 1:400).[27] The specificity of this antibody for MUC13 staining was described previously.[21, 27, 30] The stained slides were scored by a histopathologist (RL) separately in both the cytoplasm and cell membrane according to a subjective scoring systems as follows: the proportion of positive cancer cell staining was graded 0 (negative), <25% (1+), 25–50% (2+), 50–70% (3+), and >75% (4+); and the staining intensity of cancer cells was graded as weak (1+), moderate (2+), strong (3+), or very strong (4+). The

proportion and intensity scores were added to give an overall staining score for each cellular location.

Growth curves and cell viability assay

Cells (5,000 or 7,500 cells/well) were plated in a 96-well image lock plate (ESSEN BioSCIENCE, Ann Arbor, MI, USA) and visualised using a real-time cell imaging system (IncuCyte live-cell ESSEN BioSCIENCE). Growth curves were built from confluence measurements acquired during round-the-clock kinetic imaging. Cell viability was determined using MTT assays.

Migration assays

The *in vitro* cell migration rates of cells were established using the IncuCyte. Before experiments, cells were treated under the indicated conditions for 18 h. Cell migration was assessed by wound healing scratch assays, in which, RCC cells were grown to confluence and then a scratch was made using a 96-pin Wound Maker (ESSEN BioScience). The wells were washed with PBS to remove any debris and incubated in the absence of the treatment with culture medium. Wound images were automatically acquired and registered by the IncuCyte software system. Typical kinetic updates were recorded at 2 h intervals for the duration of the experiment (48 h). The data were then analysed using an integrated metric. Relative wound density was used as an indicator for wound closure.

Transwell invasion assay

Cells were seeded on the top of inserts containing an 8 micron pore size PET membrane with a thin layer of a Matrigel basement Membrane Matrix (Corning, Bedford, MA, USA) at 4.0×10^4 cells/well without serum. RPMI (600 µl) with 10% FBS was added to the lower chamber as chemoattractant. The plates were then placed in an incubator at 37°C with 5% CO2 for 24 h. After incubation, the cells remaining in the upper chamber were carefully removed, and the transwell membrane was fixed with 100% methanol and stained with 0.5% crystal violet. To count the fixed cells, images were captured randomly from 5 fields of vision at × 200 magnification.

Cell death assays

Cells were collected and incubated with LIVE/DEAD fixable dead cell stains detection kit (Life Technologies) following the manufacturer's instructions and analysed by by CytoFLEX flow

cytometry (Beckman Coulter, Brea, CA, US) using the Flowjo v10 software (Flowjo, LLC, Ashland, Oregon, US).

Immunoblot analyses

Sub-confluent cells were collected, washed with cold PBS, and harvested with cell lysate buffer (50 mM Tris, pH 7.4, 150 mM NaCl, 1.0% Triton X-100, 1x Complete protease inhibitor mixture, 2 mm sodium vanadate, 10 mm sodium fluoride). The resulting lysates were used for immunoblot analyses as described previously.[30]

Statistical analysis

Statistical analyses were performed using Prism v5 (GraphPad Software, La Jolla, CA, USA). The statistical test used and the sample sizes for individual analyses are provided within the Figure legends. Statistical significance was set at $P<0.05$.

Additional information is described in Supplementary Materials and Methods.

Results

Clinical Study Participants

A total of 244 patients from 5 distinct cohorts were included for this study (clinical data presented in Supplementary Table 1). Histologic diagnoses and tumor grading of hematoxylin and eosin-stained tissue sections were assessed according to the World Health Organization Classification of Tumours.[32] The original grading of the tumour was used for statistical purposes throughout this study, rather than the features of the individual tumour core.

MUC13 expression is associated with aggressive clear cell RCC

We initially analysed the expression profile of MUC13 by immunohistochemistry (IHC) from matched non-diseased and malignant kidney tissue. In this series of 10 ccRCC and adjacent uninvolved tissue sections (patient cohort 1), MUC13 protein expression was greater in 100% of tumors compared with adjacent non-diseased kidney (Fig.1a). In the normal kidney, MUC13 expression was restricted to the distal convoluted tubules and collecting ducts (Fig.1a, Supporting Information Figure 1A) and these cells showed uniform, membranous and cytoplasmic staining with apical polarity (Fig.1a, Supporting Information Figure 1A). No positive staining was seen elsewhere in the cortex: in particular, the glomeruli, Bowman's capsule and the proximal convoluted tubules were negative (Fig.1a, Supporting Information

Figure 1A). Increased MUC13 expression in ccRCC was validated by Western immunoblot (patient cohort 2) and qRT-PCR on an independent patient set (patient cohort 3; Figs.1b and 1c). We next expanded this MUC13 expression study to 110 distinct ccRCC patients using human tissue microarrays (patient cohort 4). MUC13 had a heterogeneous staining pattern in ccRCC, both within and between individual cancers. MUC13 was expressed in 107/110 (96%) cases of ccRCC with a predominantly diffuse cytoplasmic staining, with a minority of the cases (23/110 (20%) showing additional membranous immunoreactivity. Foci of cells staining with MUC13 were often observed in low grade cancers (Fig.1d), whereas in high grade cancers there was frequently strong cytoplasmic expression of MUC13 (Fig.1d). Using a semi quantitative score, we found that the cytoplasmic MUC13 staining score (intensity plus proportion) was significantly increased in grade III and IV tumours, compared to grade I and II tumours (Fig.1e). Together, these results suggest that MUC13 is aberrantly expressed with loss of polarization in ccRCC, and its overexpression is associated with aggressive disease whereas in normal kidney, MUC13 is present only in the collecting duct and distal tubule epithelium.

High MUC13 expression in clear cell RCC is associated with poor survival

To further determine the association of MUC13 expression with clinical outcomes, we analysed MUC13 IHC staining on tissue microarrays from two distinct cohorts (cohorts 4 and 5). Relative cytoplasmic MUC13 expression in tumor tissues from the patients was classified into two groups: low-MUC13 (low relative levels of MUC13, staining scores ≤4) and high-MUC13 (high relative levels of MUC13, scores ≥5). Long-term survival data was available from 35 ccRCC patients in Cohort 4. High-MUC13 was significantly associated with poor overall survival, with a 10-year survival of 35% compared to 91% in the low-MUC13 expression group (P = 0.011, Fig. 2a). The effect of MUC13 expression on patient survival was further assessed according to clinical stage. Approximately 55% of stage 1 tumours showed high MUC13 vs 87% of stage 2-4 tumours. Despite the small number of patients, stage 1 patients in the MUC13-high group exhibited significantly shorter survival than MUC13-low patients (10-year survival 45% and 89%, respectively; P = 0.046, Fig. 2a). The influence of MUC13 on survival in later stage disease could not be determined because only two patients had low MUC13 expression. Because MUC13 was associated with poor survival in

this small cohort, we examined MUC13 expression in a larger independent replication cohort. Cohort 5 contained 81 cases of ccRCC with long-term survival data. High-MUC13 was significantly associated with poorer overall survival, with a 5-year survival of 51% compared to 86% in the low-MUC13 expression group (P = 0.0002, Fig. 2b). The effect of MUC13 expression on patient survival was further assessed according to clinical stage. Approximately 30% of stage 1 tumours showed high MUC13 vs 59% of stage 2-4 tumours. Consistent with the finding in cohort 4, stage 1 patients in the MUC13-high group exhibited significantly shorter survival than MUC13-low patients (5-year survival 50% and 92%, respectively; P = 0.0024, Fig. 2b). MUC13 expression did not influence survival in later stage tumours (n=22), and while the numbers of late stage tumours was small, the curves were overlapping. Taken together, these findings demonstrate that MUC13 overexpression is a prognostic marker for overall survival of ccRCC patients, particularly for early stage tumours.

MUC13 overexpression in non-clear cell RCC

We next examined MUC13 expression in less prevalent histologic types of RCC, including papillary and chromophobe carcinomas. Of these 14 patients (patient cohort 4), 12 (86%) overexpressed MUC13. All eight papillary RCC showed medium to strong diffuse cytoplasmic MUC13 staining (Supporting Information Figure 2A and 2B). MUC13 expression was observed in 4 out of 6 chromophobe RCC (66%) (Supporting Information Figure 2C and 2D). Thus, MUC13 is expressed in all major histologic types of RCC.

MUC13 promotes proliferation and migration of RCC cells

To investigate the biological role of MUC13 in renal cancer, we first checked the expression of MUC13 in several ccRCC cell lines, including 769-P, 786-O, A498, A704, ACHN and Caki-1. With the exception of Caki-1 cells, all cell lines endogenously expressed MUC13 (Fig. 3a). To explore the effects of *MUC13* silencing we utilized two independent sets of siRNAs to control for potential off-target effects. Each set of *MUC13* siRNA resulted in a 68-88% reduction in MUC13 mRNA expression and protein levels 48 h post-transfection, compared with cells transfected with control siRNA (Fig. 3b). siRNA silencing of *MUC13* with either siRNA resulted in a significant decrease in cell proliferation, as measured by cell growth in real-time using an IncuCyte FLR analyser (Fig. 3c, Supporting Information Figure 3A). Further supporting a

growth promoting role, overexpression of MUC13 in HEK293 cells (Fig. 3b) enhanced their proliferation (Fig. 3c). In addition, MUC13 also promoted clonogenic potential of all cell lines as determined by colony formation assays (Fig. 3d, Supporting Information Figure 3B). Because similar results were observed with the different siRNA's (Supporting Information Figure 3A and 3B), one *MUC13* siRNA (#1 - SMART pool) was used in all subsequent experiments. Cell migration has an important role in cancer metastasis. In wound-healing experiments, we observed a marked inhibition of cell migration in 769-P and ACHN cells upon *MUC13* siRNA silencing (Fig. 3e, Supporting Information Figure 3C). The analysis of 769-P, 786-O and A498 cell invasion also demonstrated *MUC13* siRNA silencing significantly decreased the invasive properties of these tumour cells (Fig. 3f, Supporting Information Figure 3D). Taken together, these *in vitro* findings align with our clinical data associating high MUC13 expression with tumour progression and poor survival. Because another cell surface mucin, MUC1, has previously been shown to influence RCC growth[33] we checked MUC1 expression by flow cytometry in 769-P and 786-O cells and could not find MUC1 cell surface expression by flow cytometry with BC2 antibody or altered protein level of MUC1 by western blot with CT2 antibody either before or after MUC13 silencing demonstrating the specificity of our findings for MUC13 (Supporting Information Figure 4).

Silencing of MUC13 sensitises RCC cells to treatment with multi-kinase inhibitors

Given the importance of MUC13 in promoting tumorigenic properties of RCC, we investigated the effect of combining the multi-kinase inhibitors, sorafenib and sunitinib, and silencing of *MUC13* in 769-P and 786-O cells. We first silenced *MUC13* with siRNA, treated the cells with sorafenib or sunitinib, and measured cell growth, migration and apoptosis using real-time imaging and flow cytometry. Consistent with previous results, *MUC13* silencing slowed proliferation and migration, and increased apoptosis, however, in combination with sorafenib or sunitinib, silencing *MUC13* more substantially impaired cell proliferation and migration, and greatly enhanced cell death (Fig. 4a-c). These data show that *MUC13* silencing sensitises cultured RCC cells to multi-kinase inhibitors used clinically, making it a potential important target for adjuvant treatment in RCC.

MUC13 promotion of cell growth and migration is largely dependent on activation of NFκB

We next sought to determine the mechanisms by which MUC13 might govern the biology of RCC cells. To this end, we examined the effect of *MUC13* silencing on growth signalling and survival pathways. Western Blot analysis revealed that knockdown of *MUC13* alone, or in combination with sorafenib or sunitinib, decreased NFκB p65 phosphorylation, whereas exposure to sorafenib or sunitinib in the presence of MUC13 enhanced NFκB p65 phosphorylation in control siRNA-treated cells (Fig. 5a). We also examined the effect exerted on expression of proteins that regulate growth and apoptosis that are known to be downstream of NFκB. The levels of BCL-xL, survivin and cyclin D1 increased in response to sorafenib and sunitinib, and this was not seen in *MUC13*-silenced cells (Fig. 5a). These data suggest that a potential mechanism by which MUC13 enhances RCC tumour progression is via activation of NFκB and its downstream regulated gene expression. Underlining the mechanism of MUC13 action via NFκB, treatment of RCC cells with a functional inhibitor of NFκB, Bay 11-7085 (Bay), impaired survival in cells expressing MUC13 and no further effect on survival was seen when *MUC13* was silenced. Interestingly, in 769-P cells pharmacological inhibition of NFκB and *MUC13* silencing had equivalent effects, whereas in 786-O cells NFκB inhibition affected growth and survival to a greater degree than *MUC13* silencing (Fig. 5b). We also compared migration after MUC13 silencing and/or NFκB inhibition. The NFκB inhibitor (plus control siRNA) slowed migration, being equally as effective as *MUC13* siRNA in 786-O cells, with a strongly synergistic effect of the combination, and less effective than *MUC13* silencing in 769-P cells (Fig. 5c).

Silencing of MUC13 impairs cell growth and survival in sorafenib and sunitinib resistant cells

We next speculated whether *MUC13* siRNA treatment could overcome resistance in sorafenib and sunitinib resistant human RCC cells. For this purpose, we established resistant sublines (769-P sorR and 769-P sunR) from the parental 769-P cell line by eight months of culture in 2 μM sorafenib or sunitinib. 769-P sorR and 769-P sunR cells exhibited higher growth rates than the parental cells (Fig. 6a). Both resistant cell lines were unaffected by a higher dose (7 μM) of either drug (Fig. 6b). However, silencing *MUC13* in 769-P sorR and 769-P sunR cells substantially impaired cell growth and survival (Fig. 6b). Furthermore, silencing M*UC13* restored sensitivity of both resistant cell lines to sorafenib or sunitinib, as evidenced by a

decrease in cellular metabolism (MTT assay; Fig. 6b) and increased cell death (flow cytometry; Fig. 6c). Pharmacological inhibition of NFκB was less effective in 769-P sorR and 769-P sunR cells at inhibiting growth and survival than in parental cells (Fig. 6d), but *MUC13* silencing remained effective.

Because the reduced effectiveness of the NFκB inhibitor may be attributable to enhanced drug efflux in the resistant cells and given the association between MUC13 and NFκB signalling, we next attempted to elucidate whether NFκB signalling in 769-P sorR and 769-P sunR cells and the development of resistance were dependent on MUC13. Western immunoblot analysis showed that NFκB phosphorylation was greater in the resistant cells compared to their parental cell line, together with increased levels of MUC13 and BCL-xL (Fig. 6e). *MUC13* silencing alone or in combination with sorafenib or sunitinib decreased the expression of phosphorylated NFκB p65 and BCL-xL (Fig. 6f). In addition to activation of NFκB pathway, we also observed that ATP-binding cassette (ABC) transporter B1 (ABCB1 or MDR1) protein which effluxes drugs was induced by chronic sorafenib or sunitinib treatments and dependent on *MUC13* expression (Fig. 6f). Consistent with upregulation of MDR expression, chronic sorafenib or sunitinib treatments also induced resistance to a cytotoxic drug that is a MDR substrate, docetaxel, and this resistance was also dependent on *MUC13* expression (Supporting Information Figure 5). Taken together, these data show that *MUC13* is increased by sorafenib and sunitinib resistance and essential for several growth and survival mechanisms, including expression of drug efflux proteins.

Discussion

Clear cell RCC has a high metastatic rate and represents a significant and difficult-to-manage disease. Our findings with respect to the expression and function of MUC13 in ccRCC open opportunities to address several of the major challenges presented by this cancer; providing a new prognostic indicator for early stage disease and a novel therapeutic target to sensitise tumours to therapy even after the development of drug resistance.

MUC13 is expressed by virtually all RCC, with high expression positively correlated with tumor grade and poor prognosis, suggesting that MUC13 is a promising biomarker for

predicting progression. High levels of MUC13 were associated with shortened survival time, particularly for patients with TMN stage 1 disease. Thus, we propose high MUC13 expression as a prognostic biomarker for better individual risk stratification. This could identify patients who need to receive adjuvant therapy and intense follow-up after surgery; even if they are low risk according to the traditional clinicopathologic analyses. TNM staging is currently the only established pathological prognostic marker for RCC, however, despite its importance and it being widely used, there will still be questions about the validity and prognostic ability of this system alone. Therefore, MUC13 will be a promising candidate to predict the clinical outcome in patients with RCC and to select patient subgroups, which might benefit from a more personalized medicine. To translate these findings into a clinically relevant tool, further prospective studies in larger cohorts are needed and should be a priority. The association of MUC13 with poor survival bears similarity to previous findings that overexpression of MUC1 is associated with high grade, metastatic progression and poor survival in stage 1 ccRCC[34]. Relatively high MUC1 expression has also been reported in type 1 papillary renal cancers, although this was not associated with poorer survival[34]. Together with our findings this suggests that the cell surface mucin family is broadly involved in promoting RCC progression, explaining why these glycoproteins are commonly overexpressed by epithelial tumours. Although we demonstrate *in vitro* strong effects of MUC13 independent of MUC1, the relative and combined importance (where co-expressed) of these two mucins in RCC is worthy of further investigation.

In addition to the level of expression, we also observed that the pattern of immunostaining for MUC13 is different in tumour cells and normal renal tubule cells. This is also a feature of MUC13 in other cancers, where cytoplasmic accumulation of MUC13 is associated with more aggressive tumours.[23, 30] Furthermore, we show that MUC13 promotes RCC cell growth, migration and anti-apoptotic programs, consistent with previous findings regarding MUC13 in colorectal,[21] pancreatic [24, 25] and ovarian [26] cancers, and explaining the relationship with poor survival.

RNAi silencing of *MUC13* resulted in substantially decreased cell proliferation, colony formation, migration and invasion, while overexpression promoted cell growth and colony formation. In addition, *MUC13* silencing sensitised renal cancer cells to sorafenib or

sunitinib, and inhibited tumour cell migration. These findings raise the possibility that targeting MUC13 expression or function could sensitise RCC to a range of therapies, providing a new molecular target which could be combined with multiple other modalities. The development of strategies for prolonging the effects of sorafenib or sunitinib and other agents is particularly important in metastatic RCC, since these tumors typically develop resistance to therapy within 5-11 months. In elucidating the biological mechanisms by which MUC13 promotes renal cancer development, we identified similar mechanisms to those recently described in colorectal cancers. MUC13 promotes activation of the NFκB signalling pathway in RCC cells. NFκB is a central player in the behaviour of cancer cells from many types of adenocarcinoma, including RCC. NFkB promotes epithelial cancer cell growth and survival through activation of several target genes such as cyclin D1, BCL-xL and survivin, which in turn promote proliferation and/or block apoptosis. NFκB inhibition had a potent effect on the RCC cells and the influence of MUC13 on cell growth/survival was lost. Targeting NFκB directly is problematic because of its many roles in normal cells and therefore MUC13 provides a target which phenocopies NFκB inhibition but has greater tumour specificity. These data further strength a model in which MUC13–induced cell proliferation, migration and –inhibition of apoptosis is mediated through the NFκB pathway across multiple cancer types.

Sunitinib has been shown to effectively inhibit neovascularization and produce antitumor effects, but in mice with pancreatic neuroendocrine tumours, adaptation to sunitinib can lead to development of increased invasion and metastasis.[36] Consistent with this preclinical finding, the majority of patients who receive sunitinib for advanced ccRCC exhibit progressive disease within one year of treatment.[37] We show that chronic exposure to sunitinib or sorafenib promoted RCC cell growth and developed drug resistance. This drug resistance was associated with increased expression of MUC13, and both resistant sublines remained sensitive to MUC13 silencing, with increased cell death and inhibition of proliferation. These findings suggest that MUC13 is an important mediator of drug resistance and that MUC13 remains a viable target in drug resistant cancers.

The mechanism of *MUC13* silencing in reducing resistance to standard anti-angiogenic therapeutic agents may be multifactorial. The effect of MUC13 in promoting drug resistance may be attributed to its ability to drive NFκB activation which has previously been

shown to be a regulator of the drug transporter pump ABCB1/MDR1. This pathway provides a mechanism additional to effects on proliferation and apoptosis by which the MUC13-NFκB axis promotes resistance to therapy. We believe selective inhibition of MUC13 expression is a promising strategy. Minimal side effects have been demonstrated in treating colorectal cancer [30] and inhibition of MUC13 may also prove effective in ccRCC. Here, we report for the first time that MUC13 silencing in combination with sorafenib and sunitinib, current therapy for RCC, not only enhances the sensitivity of naïve RCC cell lines to sorafenib and sunitinib, but also reverses sorafenib and sunitinib resistance in resistant cell lines. We provide the rationale and experimental evidence for the combined use of MUC13 antagonism and sorafenib or sunitinib to potentially limit and overcome drug resistance in patients with MUC13–overexpressing RCC. In conclusion, these data suggest that MUC13 may be a useful prognostic biomarker and potential therapeutic target in RCC, with the potential to lead to better outcomes for patients with these poor prognosis malignancies.

Acknowledgments

This work was supported by NHMRC project grant 1060698 and by funding from the Mater Foundation, MAM is supported by a NHMRC Senior Research Fellowship. RL was partly supported by a Betty McGrath/Mater Practitioner Research Fellowship. IS is supported by a QUT Vice-Chancellor's Senior Research Fellowship. The Translational Research Institute (TRI) is supported by a grant from the Australian Government. We acknowledge Prof. Hemamali Samaratunga, Aquesta Specialised Uropathology as consultant for histopathology of RCC. We also recognize the technical assistance of the TRI core facilities for histology, flow cytometry and microscopy.

Figure legends

Figure 1. MUC13 is aberrantly overexpressed in clear cell renal cell carcinomas and associated with aggressive disease. (a) Two representative photomicrographs of MUC13 immunohistochemical (IHC) staining of kidney sections showing ccRCC and adjacent normal kidney. (b) MUC13 protein level determined by Western blotting in a panel of 8 RCC tumours (T) and adjacent normal (N) kidney tissues. Patients 1-4, 6 and 7 are ccRCC, patients 5 and 8 are papillary RCC. Densitometry analysis of MUC13 corrected for β-actin is shown in the right panel. (c) *MUC13* mRNA expression in ccRCC vs normal kidney (corrected for β-actin, fold of mean of normal tissue). (d) Representative photomicrographs of MUC13 IHC staining in low and high grade ccRCC: (i) Weak MUC13 staining in grade I ccRCC; (ii) MUC13 showing a mixed circumferential membranous and diffuse cytoplasmic expression in grade II ccRCC; (iii) MUC13 showing a strong diffuse cytoplasmic expression in grade III ccRCC; (iv) MUC13 showing a strong intense diffuse cytoplasmic expression in grade IV ccRCC. (e) MUC13 cytoplasmic protein levels (the score of intensity plus proportion, see methods) assessed on a tissue microarray by immunohistochemistry of ccRCC (n = 110) classified by tumor grade. Statistics: (b, c and e) mean ± SEM. Mann-Whitney U-test, * vs normal (b,c) or vs grade I tumor , # vs grade II tumor, + vs grade III tumor (E), *,# $p < 0.05$, ## $p < 0.001$, ***,### $p < 0.0001$

Figure 2. High MUC13 expression in clear cell RCC is associated with poor survival. Kaplan-Meier curves for overall survival in two independent cohorts of patients with ccRCC according to expression of MUC13. (a) Overall survival in patients cohort 4 with low or high level MUC13 determined by IHC (b) Overall survival in patients cohort 5 with low or high level MUC13 determined by IHC. Statistics: Log-rank *P*-values shown where significant.

Figure 3. MUC13 promotes RCC cell proliferation, migration and colony formation. (a) *MUC13* mRNA levels were measured by qRT-PCR; expressed as fold of HEK293 (corrected for β-actin) in a panel of ccRCC cell lines. (b) Knockdown of MUC13 in the indicated cell lines 48 h after transfection with control (-) siRNA (Ctl siR) or *MUC13* siRNA #1 (*M13* siR #1-SMART pool) or *MUC13* siRNA #2 (*M13* siR #2 – *MUC13* 13:1) was assessed by Western blot and qRT-PCR. Densitometric measurements were normalised to β-actin and expressed as % of control siRNA, and reported under western blot images. Expression of MUC13 in HEK293 cells by stably transduced retrovirus infection with a control (-) vector or MUC13 (+) expression vector was assessed by by Western blot and qRT-PCR. Densitometric measurements were normalised to β-actin and expressed as % of control vector, and reported under western blot images. (c) Cell growth in real time was monitored using an IncuCyte FLR live cell imager in the indicated RCC cells with MUC13 knockdown (*MUC13* siRNA #1), or control and *MUC13* over-expressing HEK293 cells. Data analysed using IncuCyte confluence v 1.5. Mean ± SD (n=4). (d) The indicated RCC cells which were transfected with control or *MUC13* siRNA, or control and *MUC13* over-expressing HEK293 cells were analysed by colony formation. Cell colonies were stained with crystal violet and counted at the end of the experiments. Representative pictures of the whole plates and relative colony numbers plotted are shown (n=4 or 6). (e) Wound healing assay in control and *MUC13* siRNA transfected 769-P cells. The gap distances were marked by the software with a yellow line and percent of wound closure was measured by using an IncuCyte FLR live cell imager. Representative pictures of the cell migration at 0, 14 and 48 h are shown (n=4). (f) Cell Invasion of control and *MUC13* siRNA transfected 769-P, and 786-O cells was evaluated using 24-well Matrigel invasion chambers with 10% fetal calf serum as chemoattractant. Representative images of the invaded cell through Matrigel-coated membranes are shown in the left. The graphs show the relative number of invasive cells counted 24 h after seeding (n=4). (a-f) The data are representative of three independent experiments. Statistics: (b, d) mean ± SEM, (e, f) box plots show median, quartiles, and range; Mann-Whitney U-test, * vs control siRNA, *$p < 0.05$.

Figure 4. Silencing of MUC13 sensitises RCC cells to treatment with sorafenib and sunitinib. (a) 769-P and 786-O cells were transfected with control (Ctl siR) or *MUC13* siRNA (M13 siR). After 24 h cells 5,000 cells/well were seeded into 96-well plates and treated with 7 μM sorafenib or 7 μM sunitinib, or vehicle for 100 h. Real time imaging was conducted in an IncuCyte FLR live cell imager. (b*)* 769-P and 786-O cells were transfected as in (A), grown to reach confluence, and exposed to 7 μM sorafenib or 7 μM sunitinib, or vehicle for 18 h prior to scratching the monolayer and monitoring wound repair with the incuCyte as in Fig 2E. (c) 769-P and 786-O cells were transfected as in (a). After 24 h 100,000 cells/well were seeded into 12-well plates and treated with 7 μM sorafenib or 7 μM sunitinib, or vehicle for a further 24 h. Representative flow cytometry plots of cells stained with live and dead dye and the percentage of cell death determined by flow cytometry are shown. (a-c) The data are representative of three independent experiments. Statistics: (c) box plots show median, quartiles, and range; mann-Whitney U-test, * vs control siR with same treatment, $^{\#}$ vs *MUC13* siR untreated, $^{*,\#}$ $p < 0.05$.

Figure 5. Promotion of cell growth and migration by MUC13 is largely dependent on activation of NFκB. (a) 769-P and 786-O cells were transfected with control or *MUC13* siRNA for 24 h, and then treated with 3.5 μM sorafenib or 3.5 μM sunitinib, or vehicle for a further 48 h. Whole cell extracts were analysed by immunoblot with the indicated antibodies. (b) 769-P and 786-O cells were transfected with control or *MUC13* siRNA for 24 h, and then treated with Bay 117805 (Bay) (4 μM) for a further 48 h. Live cell activity in the cultures was determined by measuring MTT and expressed as % of cells treated with control siRNA and vehicle control**.** (c) 769-P and 786-O cells were transfected as in (a)*,* grown to reach confluence, and exposed to 4 μM Bay or vehicle for 18 h prior to scratching the monolayer and monitoring wound repair with the incuCyte as per Fig 2E. (a-c) The data are representative of three independent experiments.Statistics: (b) mean ± SEM, n = 4. Mann-Whitney U-test, * vs control with same treatment or as indicated, *, $p < 0.05$.

Figure 6. MUC13 silencing reverses sorafenib and sunitinib resistance. (a) 769-P sorafenib-resistant (sorR), 769-P sunitinib-resistant (sunR) and the parental 769-P cell lines were seeded at 5,000 cells/well in 96-well plate and real time imaging was conducted in an IncuCyte FLR live cell imager. (b) 769-P sorR, 769-P sunR cells were transfected with control or *MUC13* siRNA for 24 h, and then treated for a further 48 h with either 7 μM sorafenib or 7 μM sunitinib, or vehicle. Live cell activity in the cultures was determined by measuring MTT and expressed as % of cells treated with control siRNA and vehicle control. (c) 769-P sorR and 769-P sunR cells were transfected and treated as in (b). Representative flow cytometry plots of cells stained with live and dead dye and the percentage of cell death determined by flow cytometry was shown. (d) 769-P sorR, 769-P sunR and the parental 769-P cell lines were transfected as in (b). After 24 h 5,000 cells/well were seeded into 96-well plates and treated with 4 μM Bay 117085. Real time imaging was conducted in an IncuCyte FLR live cell imager. (e) Whole cell extracts from 769-P sorR and 769-P sunR resistant cell lines were analysed by immunoblot with the indicated antibodies. (f) 769-P sorR and 769-P sunR and the parental 769-P cell lines were transfected with control or *MUC13* siRNA for 48 h, and then whole cell extracts were analysed by immunoblot with the indicated antibodies. Statistics: (b, c) box plots show median, quartiles, and range; n = 4. Mann-Whitney U-test, * vs control siRNA with same treatment or as indicated, $^{\#}$ vs *MUC13* siRNA untreated, $^{*,\#}$ $p < 0.05$.

References:

1. Campbell SC, Flanigan RC, Clark JI. Nephrectomy in metastatic renal cell carcinoma. Curr. Treat. Options Oncol. 2003;4:363-72.

2. Ferlay J, Soerjomataram I, Dikshit R, Eser S, Mathers C, Rebelo M, Parkin DM, Forman D, Bray F. Cancer incidence and mortality worldwide: sources, methods and major patterns in GLOBOCAN 2012. Int. J. Cancer 2015;136:E359-86.

3. Lopez-Beltran A, Scarpelli M, Montironi R, Kirkali Z. 2004 WHO classification of the renal tumors of the adults. Eur. Urol. 2006;49:798-805.

4. McDermott DF, Regan MM, Clark JI, Flaherty LE, Weiss GR, Logan TF, Kirkwood JM, Gordon MS, Sosman JA, Ernstoff MS, Tretter CP, Urba WJ, et al. Randomized phase III trial of high-dose interleukin-2 versus subcutaneous interleukin-2 and interferon in patients with metastatic renal cell carcinoma. J. Clin. Oncol. 2005;23:133-41.

5. Griffioen AW, Mans LA, de Graaf AM, Nowak-Sliwinska P, de Hoog CL, de Jong TA, Vyth-Dreese FA, van Beijnum JR, Bex A, Jonasch E. Rapid angiogenesis onset after discontinuation of sunitinib treatment of renal cell carcinoma patients. Clin. Cancer Res. 2012;18:3961-71.

6. Haas NB, Manola J, Uzzo RG, Flaherty KT, Wood CG, Kane C, Jewett M, Dutcher JP, Atkins MB, Pins M, Wilding G, Cella D, et al. Adjuvant sunitinib or sorafenib for high-risk, non-metastatic renal-cell carcinoma (ECOG-ACRIN E2805): a double-blind, placebo-controlled, randomised, phase 3 trial. Lancet 2016;387:2008-16.

7. McAuley JL, Linden SK, Png CW, King RM, Pennington HL, Gendler SJ, Florin TH, Hill GR, Korolik V, McGuckin MA. MUC1 cell surface mucin is a critical element of the mucosal barrier to infection. J. Clin. Invest. 2007;117:2313-24.

8. Sheng YH, Hasnain SZ, Florin TH, McGuckin MA. Mucins in Ibd and Colorectal Cancer. J. Gastroenterol. Hepatol. 2011;27:28-38.

9. McGuckin MA, Linden SK, Sutton P, Florin TH. Mucin dynamics and enteric pathogens. Nat Rev Microbiol 2011;9:265-78.

10. Jonckheere N, Skrypek N, Van Seuningen I. Mucins and tumor resistance to chemotherapeutic drugs. Biochim. Biophys. Acta 2014;1846:142-51.

11. Nath S, Mukherjee P. MUC1: a multifaceted oncoprotein with a key role in cancer progression. Trends Mol. Med. 2014;20:332-42.

12. Andrianifahanana M, Moniaux N, Schmied BM, Ringel J, Friess H, Hollingsworth MA, Buchler MW, Aubert JP, Batra SK. Mucin (MUC) gene expression in human pancreatic adenocarcinoma and chronic pancreatitis: a potential role of MUC4 as a tumor marker of diagnostic significance. Clin. Cancer Res. 2001;7:4033-40.

13. Hollingsworth MA, Strawhecker JM, Caffrey TC, Mack DR. Expression of MUC1, MUC2, MUC3 and MUC4 mucin mRNAs in human pancreatic and intestinal tumor cell lines. Int. J. Cancer 1994;57:198-203.

14. McDermott KM, Crocker PR, Harris A, Burdick MD, Hinoda Y, Hayashi T, Imai K, Hollingsworth MA. Overexpression of MUC1 reconfigures the binding properties of tumor cells. Int. J. Cancer 2001;94:783-91.

15. Swartz MJ, Batra SK, Varshney GC, Hollingsworth MA, Yeo CJ, Cameron JL, Wilentz RE, Hruban RH, Argani P. MUC4 expression increases progressively in pancreatic intraepithelial neoplasia. Am. J. Clin. Pathol. 2002;117:791-6.

16. Kufe DW. Mucins in cancer: function, prognosis and therapy. Nat. Rev. Cancer 2009;9:874-85.

17. Kufe DW. MUC1-C oncoprotein as a target in breast cancer: activation of signaling pathways and therapeutic approaches. Oncogene 2013;32:1073-81.

18. Hollingsworth MA, Swanson BJ. Mucins in cancer: protection and control of the cell surface. Nat. Rev. Cancer 2004;4:45-60.

19. Kufe DW. Functional targeting of the MUC1 oncogene in human cancers. Cancer Biol. Ther. 2009;8:1197-203.

20. Shimamura T, Ito H, Shibahara J, Watanabe A, Hippo Y, Taniguchi H, Chen Y, Kashima T, Ohtomo T, Tanioka F, Iwanari H, Kodama T, et al. Overexpression of MUC13 is associated with intestinal-type gastric cancer. Cancer Sci. 2005;96:265-73.

21. Walsh MD, Young JP, Leggett BA, Williams SH, Jass JR, McGuckin MA. The MUC13 cell surface mucin is highly expressed by human colorectal carcinomas. Hum. Pathol. 2007;38:883-92.

22. Gupta BK, Maher DM, Ebeling MC, Stephenson PD, Puumala SE, Koch MR, Aburatani H, Jaggi M, Chauhan SC. Functions and regulation of MUC13 mucin in colon cancer cells. J. Gastroenterol. 2014;49:1378-91.

23. Gupta BK, Maher DM, Ebeling MC, Sundram V, Koch MD, Lynch DW, Bohlmeyer T, Watanabe A, Aburatani H, Puumala SE, Jaggi M, Chauhan SC. Increased expression and aberrant localization of mucin 13 in metastatic colon cancer. J. Histochem. Cytochem. 2012;60:822-31.

24. Khan S, Ebeling MC, Zaman MS, Sikander M, Yallapu MM, Chauhan N, Yacoubian AM, Behrman SW, Zafar N, Kumar D, Thompson PA, Jaggi M, et al. MicroRNA-145 targets MUC13 and suppresses growth and invasion of pancreatic cancer. Oncotarget 2014;5:7599-609.

25. Chauhan SC, Ebeling MC, Maher DM, Koch MD, Watanabe A, Aburatani H, Lio Y, Jaggi M. MUC13 Mucin Augments Pancreatic Tumorigenesis. Mol. Cancer Ther. 2012;11:24-33.

26. Chauhan SC, Vannatta K, Ebeling MC, Vinayek N, Watanabe A, Pandey KK, Bell MC, Koch MD, Aburatani H, Lio Y, Jaggi M. Expression and functions of transmembrane mucin MUC13 in ovarian cancer. Cancer Res. 2009;69:765-74.

27. Williams SJ, Wreschner DH, Tran M, Eyre HJ, Sutherland GR, McGuckin MA. MUC13, a novel human cell surface mucin expressed by epithelial and hemopoietic cells. Journal of Biological Chemistry 2001;276:18327-36.

28. Linden SK, Sutton P, Karlsson NG, Korolik V, McGuckin MA. Mucins in the mucosal barrier to infection. Mucosal Immunology 2008;1:183-97.

29. Sheng YH, Lourie R, Linden SK, Jeffery PL, Roche D, Tran TV, Png CW, Waterhouse N, Sutton P, Florin TH, McGuckin MA. The MUC13 cell-surface mucin protects against intestinal inflammation by inhibiting epithelial cell apoptosis. Gut 2011;60:1661-70.

30. Sheng YH, He Y, Hasnain SZ, Wang R, Tong H, Clarke DT, Lourie R, Oancea I, Wong KY, Lumley JW, Florin TH, Sutton P, et al. MUC13 protects colorectal cancer cells from death by activating the NF-kappaB pathway and is a potential therapeutic target. Oncogene 2016:doi 10.1038/onc.2016.241. Advance online publication 11 July 2016.

31. Sheng YH, Triyana S, Wang R, Das I, Gerloff K, Florin TH, Sutton P, McGuckin MA. MUC1 and MUC13 differentially regulate epithelial inflammation in response to inflammatory and infectious stimuli. Mucosal Immunol. 2013;6:557-68.

32. Delahunt B, Cheville JC, Martignoni G, Humphrey PA, Magi-Galluzzi C, McKenney J, Egevad L, Algaba F, Moch H, Grignon DJ, Montironi R, Srigley JR, et al. The International Society of Urological Pathology (ISUP) grading system for renal cell carcinoma and other prognostic parameters. Am. J. Surg. Pathol. 2013;37:1490-504.

33. Bouillez A, Gnemmi V, Gaudelot K, Hemon B, Ringot B, Pottier N, Glowacki F, Butruille C, Cauffiez C, Hamdane M, Sergeant N, Van Seuningen I, et al. MUC1-C nuclear localization drives invasiveness of renal cancer cells through a sheddase/gamma secretase dependent pathway. Oncotarget 2014;5:754-63.

34. Leroy X, Zerimech F, Zini L, Copin MC, Buisine MP, Gosselin B, Aubert JP, Porchet N. MUC1 expression is correlated with nuclear grade and tumor progression in pT1 renal clear cell carcinoma. Am. J. Clin. Pathol. 2002;118:47-51.

35. Leroy X, Zini L, Leteurtre E, Zerimech F, Porchet N, Aubert JP, Gosselin B, Copin MC. Morphologic subtyping of papillary renal cell carcinoma: correlation with prognosis and differential expression of MUC1 between the two subtypes. Mod. Pathol. 2002;15:1126-30.

36. Paez-Ribes M, Allen E, Hudock J, Takeda T, Okuyama H, Vinals F, Inoue M, Bergers G, Hanahan D, Casanovas O. Antiangiogenic therapy elicits malignant progression of tumors to increased local invasion and distant metastasis. Cancer Cell 2009;15:220-31.

37. Rini BI, Flaherty K. Clinical effect and future considerations for molecularly-targeted therapy in renal cell carcinoma. Urol. Oncol. 2008;26:543-9.

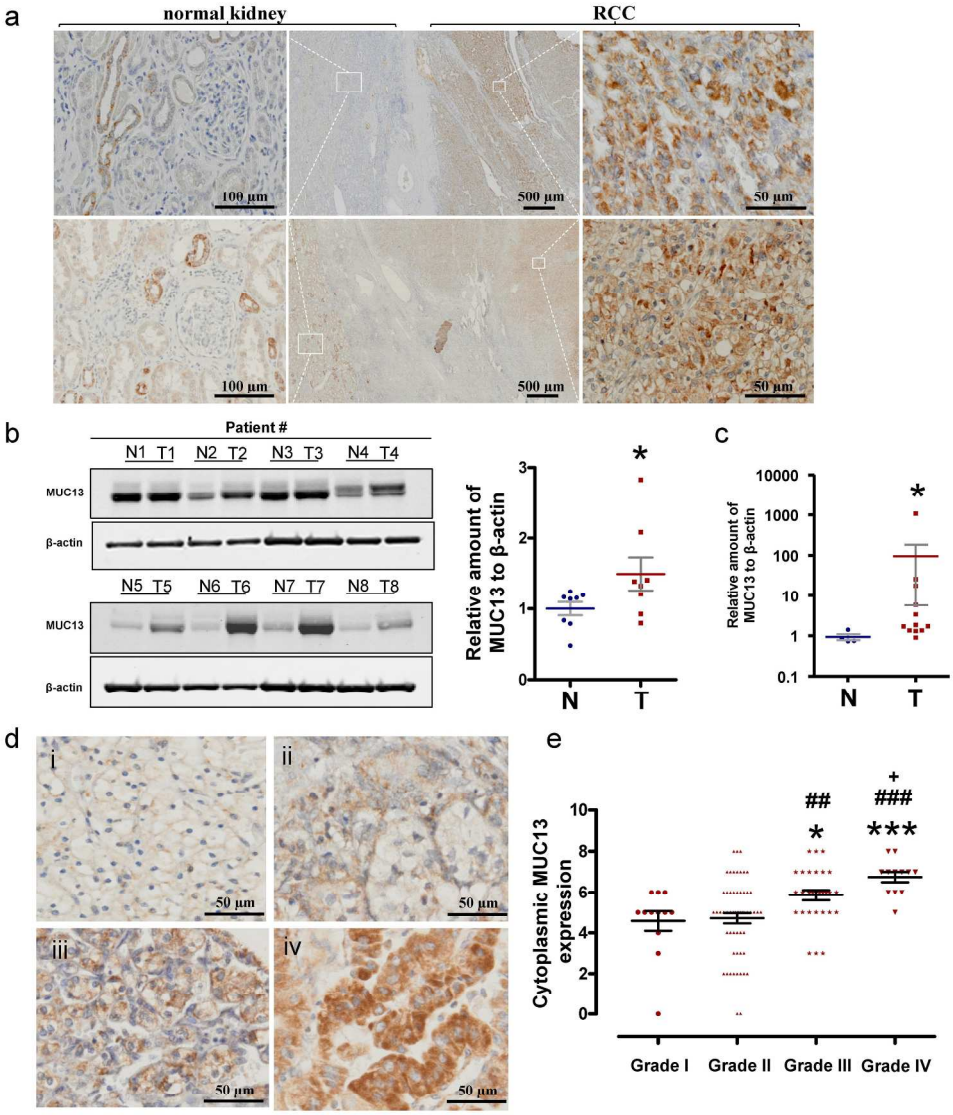

Figure 1

Figure 1
235x284mm (300 x 300 DPI)

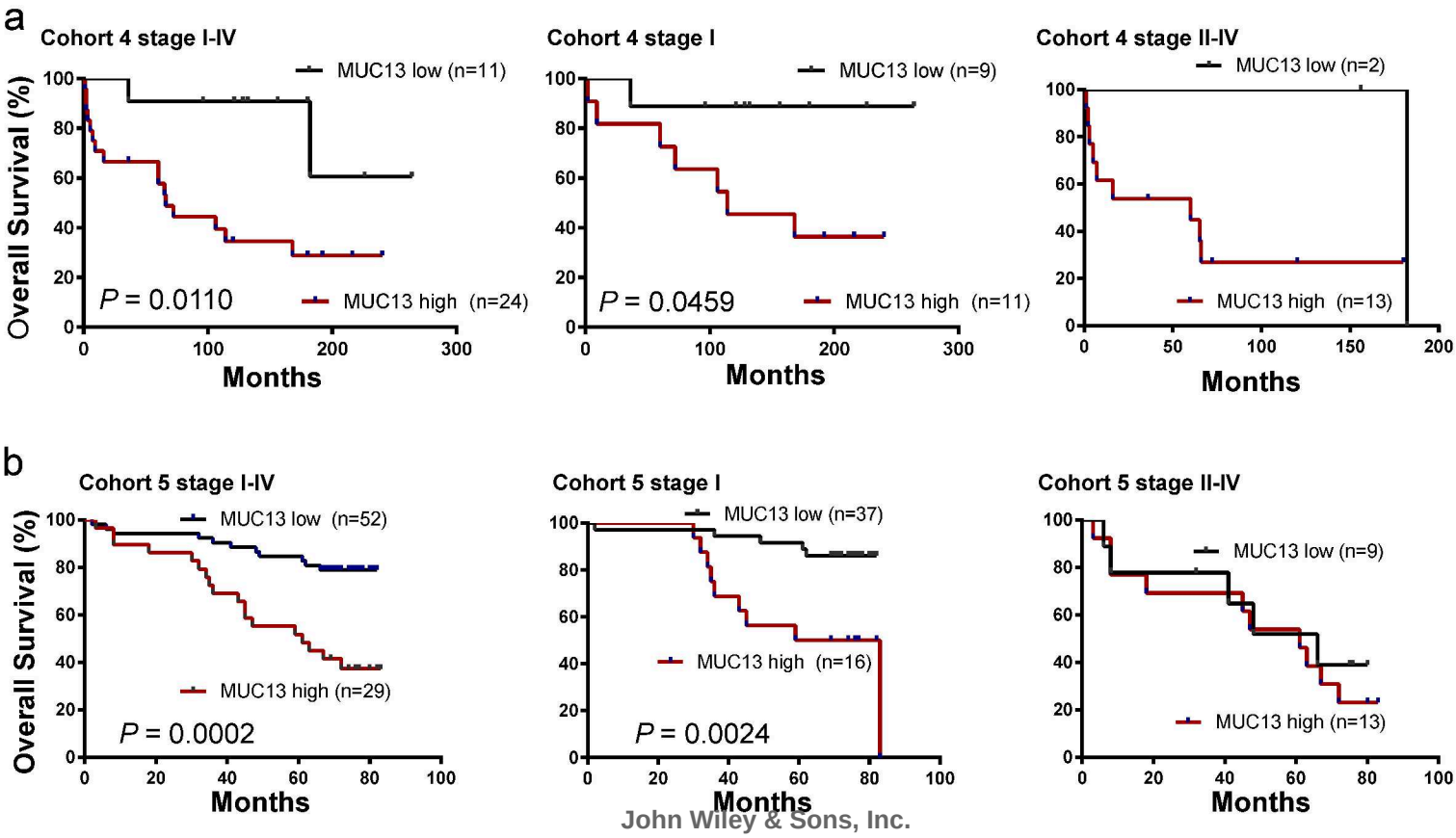

Figure 2

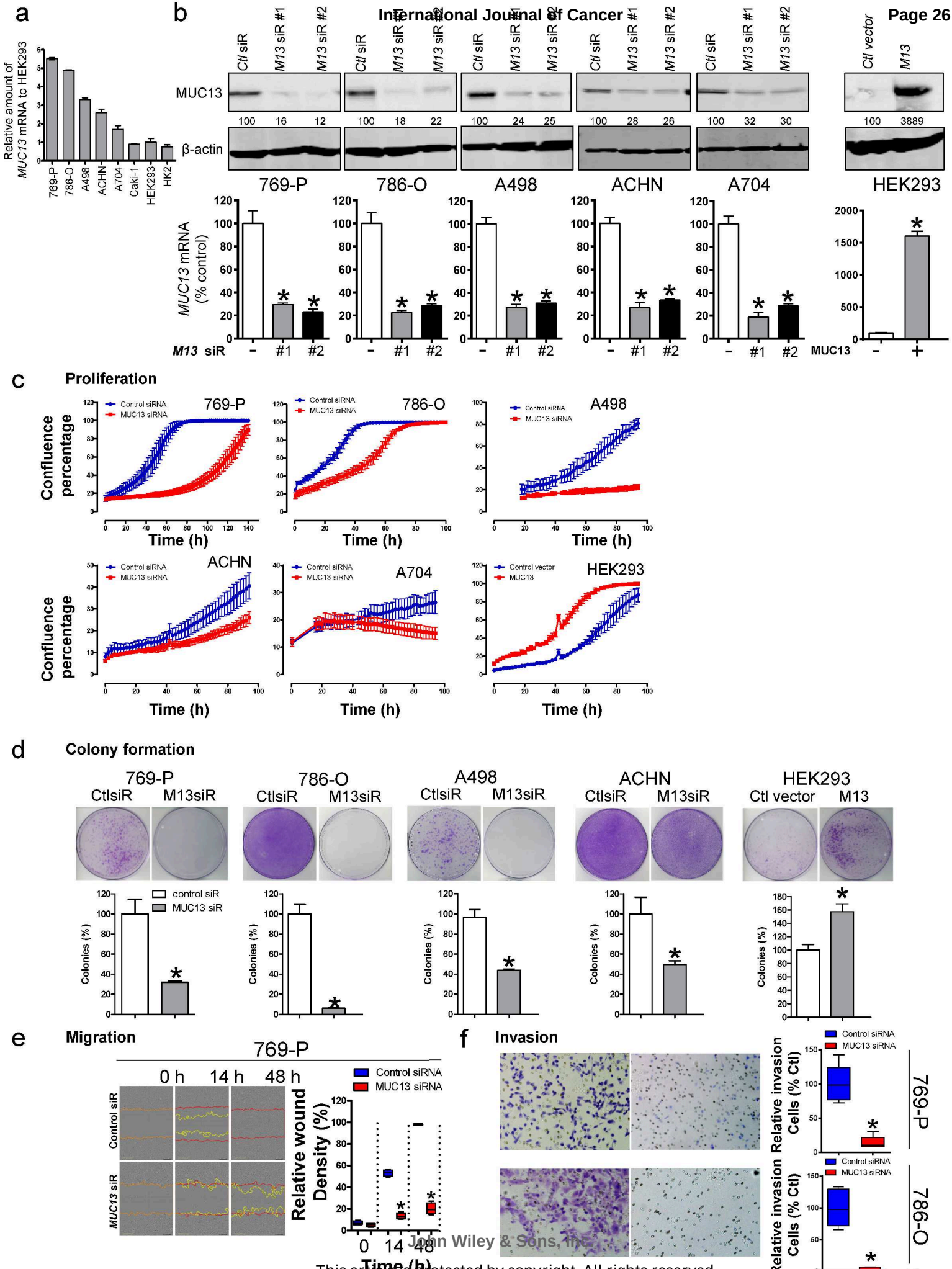

Figure 3

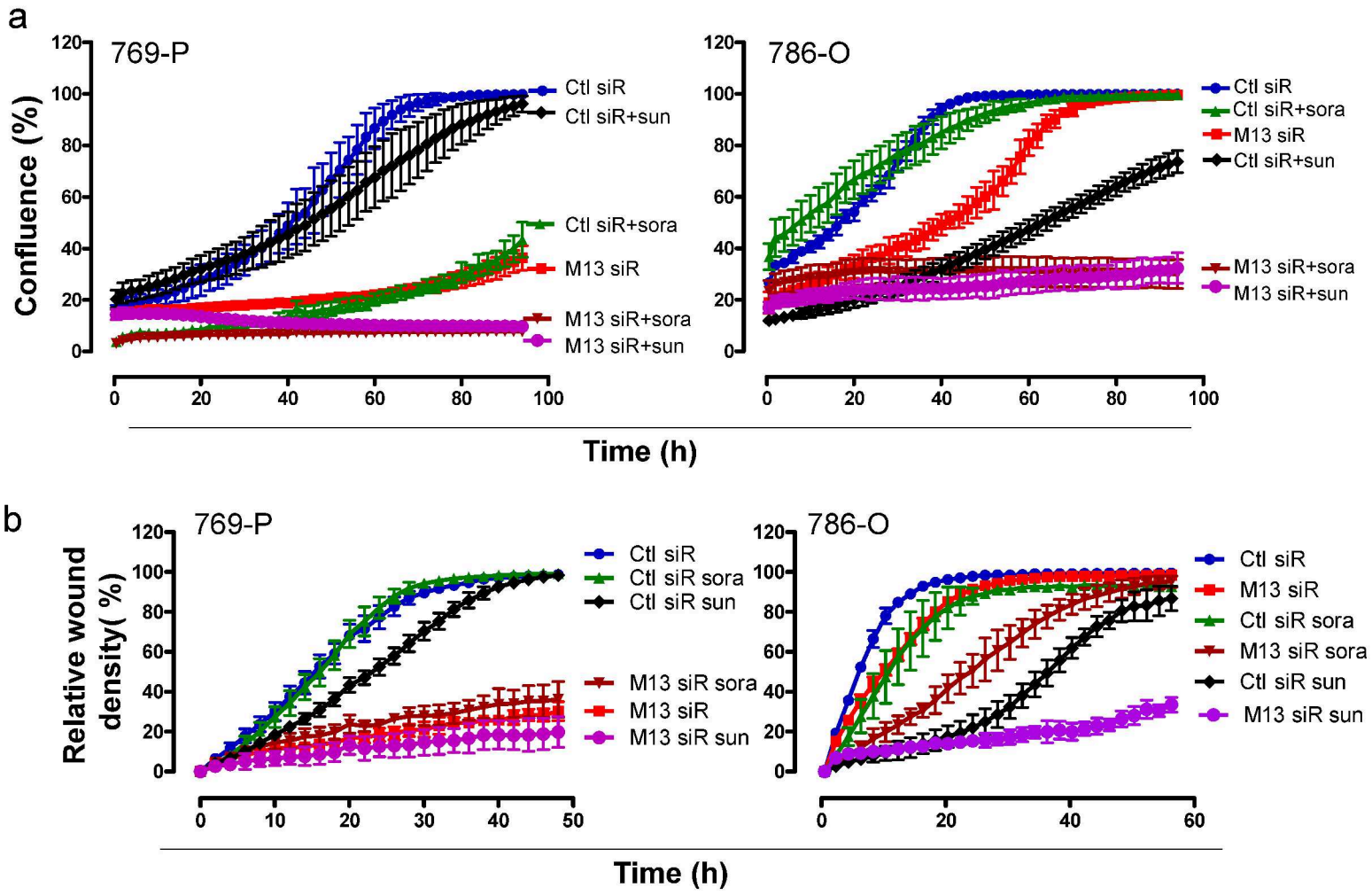

Figure 4

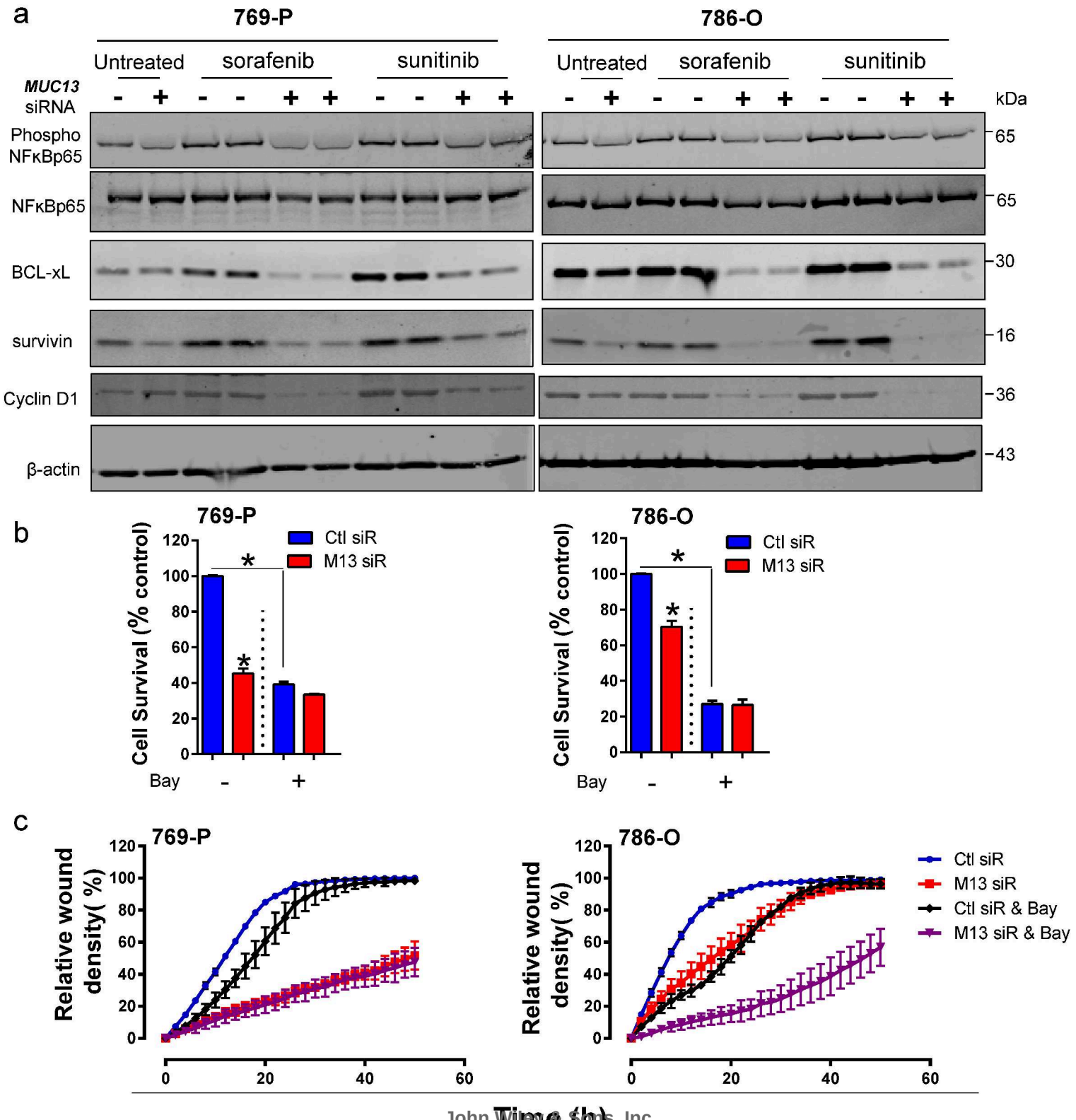

Figure 5

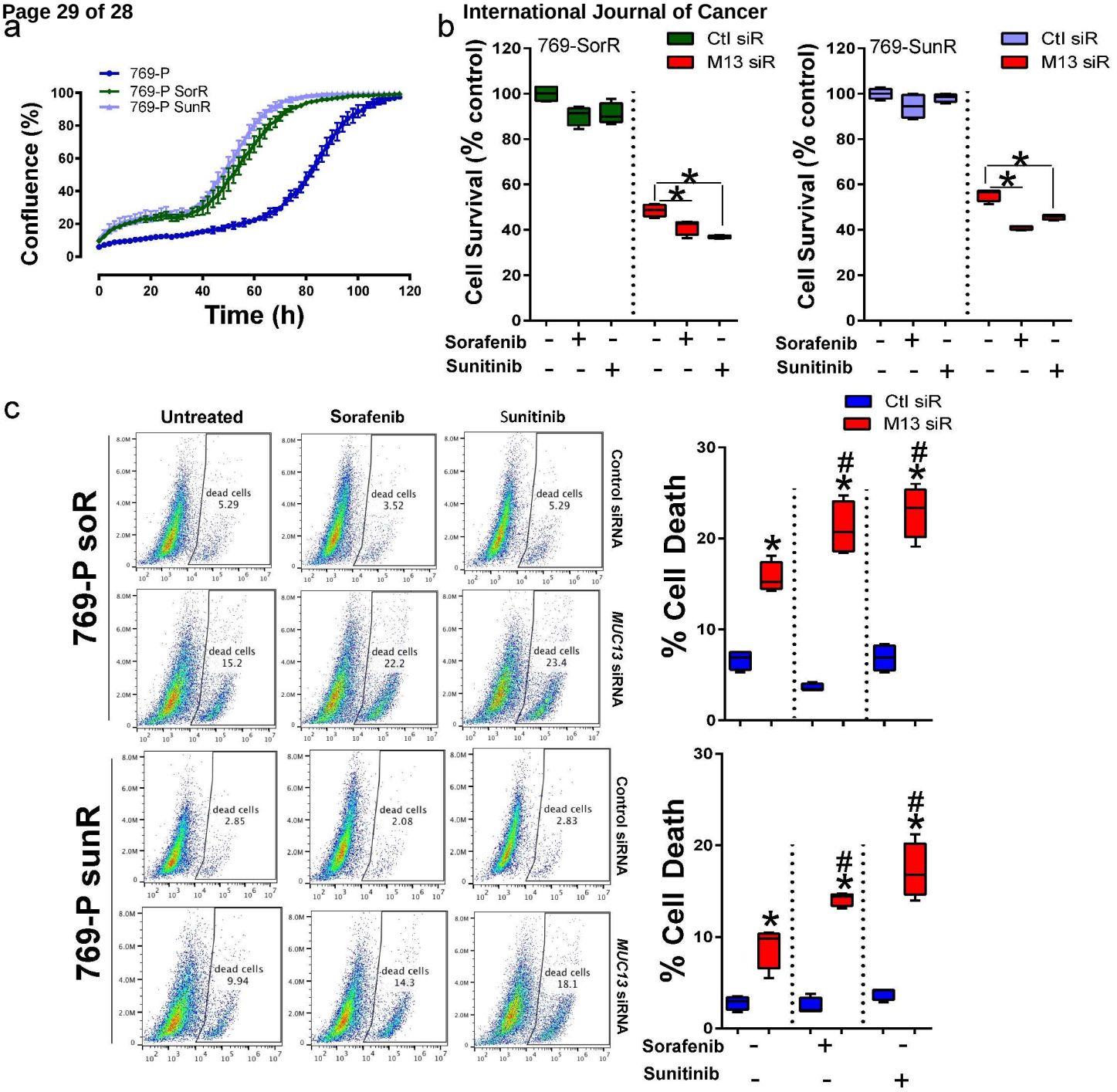

Figure 6